Supporting information for Self-assembled layering of magnetic nanoparticles in a ferrofluid at silicon surfaces

Katharina Theis-Bröhl,[*,†] Erika C. Vreeland,[‡,¶] Andrew Gomez,[‡] Dale L. Huber,[‡] Apurve Saini,[§] Max Wolff,[§] Brian B. Maranville,[∥] Erik Brok,[∥,⊥] Kathryn L. Krycka,[∥] Joseph A. Dura,[∥] and Julie A. Borchers[∥]

†*University of Applied Sciences, An der Karlstadt 8, 27568 Bremerhaven, Germany*

‡*Sandia National Laboratories, Albuquerque, New Mexico, 87185*

¶*Imagion Biosystems LLC, Albuquerque, New Mexico, 87106*

§*Division for Materials Physics, Uppsala University, 75120 Uppsala, Sweden*

∥*NIST Center for Neutron Research, 100 Bureau Drive, Gaithersburg, MD 20899-6102*

⊥*Department of Materials Science and Engineering, University of Maryland, MD-20742, College Park*

E-mail: ktheisbroehl@hs-bremerhaven.de

Phone: +49 471 4823471

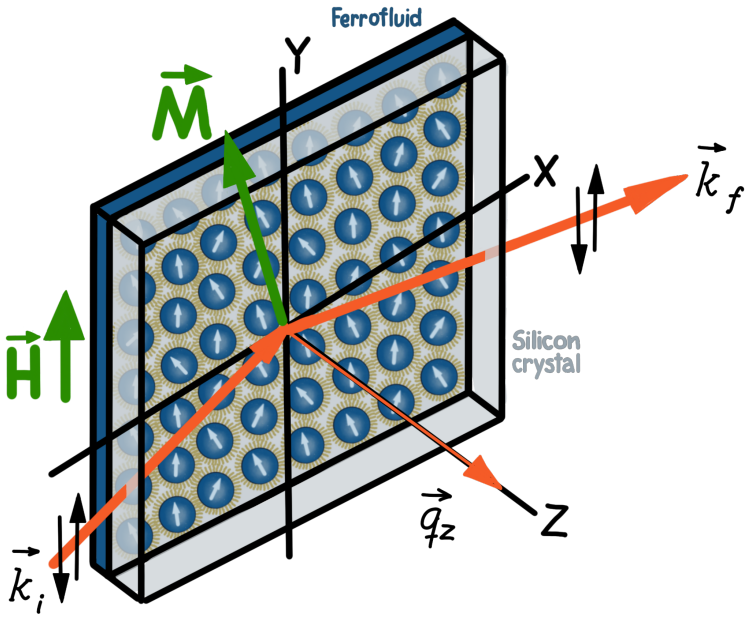

Figure S1: Sketch of the experimental setup showing the incident and reflected neutron beams (k_i, k_f) and the sample assembly. q_z is the vector of momentum transfer perpendicular to the interface.

Neutron reflectivity

Scattering geometry

The scattering geometry used for the neutron reflectivity experiments is shown in Figure S1. The polarized neutron beam penetrates the silicon crystal and is scattered at the silicon/ferrofluid interface. The reflected neutron beam again travels through the silicon crystal towards the detector.

Results of unpolarized neutron reflectivity measurements

Figure S2 shows the unpolarized NR data taken at 0 mT (left) and 100 mT (right) in which $R \cdot q_z^4$ is plotted as function of q_z and uncertainties which are $\pm$ one standard deviation. The

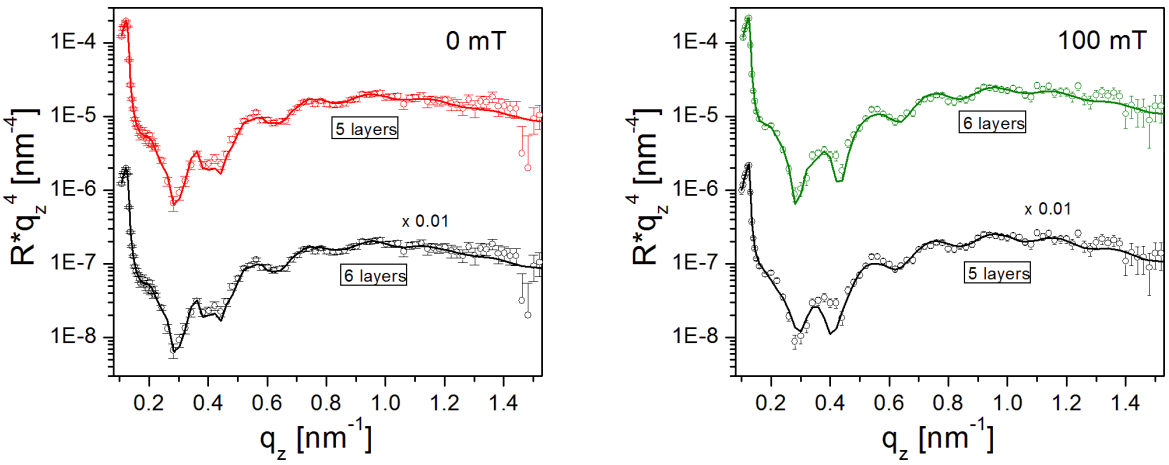

Figure S2: NR data taken in zero field (left) and in a field of 100 mT (right). Shown are plots of $R \cdot q_z^4$ as function of q_z. The solid lines represent fits to the data. Each plot shows the best fits to a model with 5 and 6 layers, shifted with respect to each other by a factor of 0.01.

measured reflectivities show pronounced deviations from the Fresnel curve, $R \propto q_z^{-4}$. For determining the optimal number of layers in our model, we performed fits with 3-6 layers between Si/SiO_2 and the bulk ferrofluid. Our analysis indicated that the data taken at 0 mT are best fit with 5 layers while the data taken at 100 mT are best fit with 6 layers. The best fits to the data are shown as solid lines in Figure S2. The resulting $Nb = f(z)$ SLD profiles are plotted in Figure S3. Since the main differences in the models are in layer # 4 (i.e., it splits into two layers at high magnetic field), we compare fits in Figure S2 with 5 and 6 layers each. Both models fit the 0 mT data with $\chi^2 = 1.3$, and the resulting $Nb = f(z)$ SLD profiles are nearly identical. In contrast, the fit to the 100 mT data using a model with 6 layers is significantly better ($\chi^2 = 1.3$, BIC=140) than the best fit using a model with 5 layers ($\chi^2 = 2.5$, BIC=239). The values for thickness, roughness and nuclear SLDs plotted in Figure S3 are given in Table S1. In both magnetic field cases we find that nanoparticles wetting the silicon surface. This wetting layer consists of the three slabs #1-3 of the stack which were defined in our model shown in the main part of the paper. Slab #2 contains the cores (and shells between the particles within this layer) and slabs #1 and #3 are layers

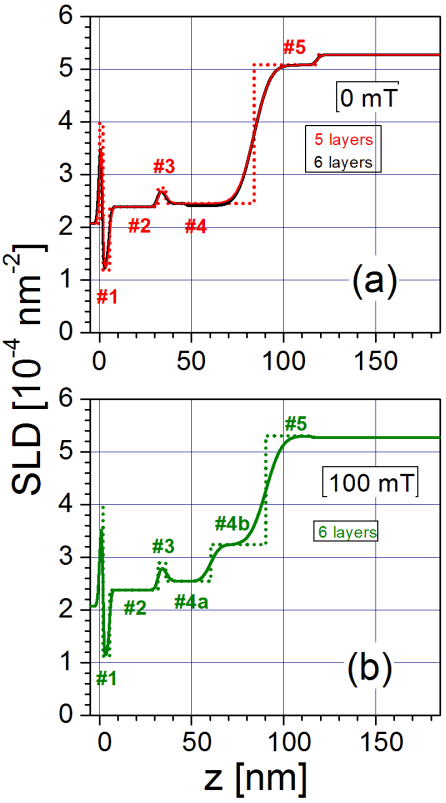

Figure S3: Profile of nuclear $Nb(z)$ scattering length density plotted as function of distance z from the Si (100) surface determined from results of fitting routines applied to the NR data shown in Figure S2.

containing mostly shell material. Slab #1 is directly attached to the silicon surface. Further layering was found on top of the first nanoparticle wetting layer. Slab #5 close to the bulk ferrofluid basically was necessary for accounting for a magnetic moment at the interface to the bulk ferrofluid which does not carry a detectable magnetic moment itself. Its nuclear SLD does not deviate much from that of the ferrofluid. Therefore, it was not necessary to include such a layer in models for the unpolarized data. For consistency, however, we used the same number of layers. In between the wetting layer and the magnetic layer at the interface to the bulk ferrofluid, either one layer (#4 in zero field) or two single layers (#4a and #4b in high field) with different SLDs build up.

Table S1: Thickness, roughness and nuclear SLD parameters obtained from fits to the NR data taken in magnetic fields of H=0 mT and H=100 mT.

Layer	$H = 0$ mT $\chi^2 = 1.3$			Layer	$H = 100$ mT $\chi^2 = 1.3$		
	Thickness t [nm]	Roughness Δt [nm]	Nuclear SLD Nb [10^{-4}nm^{-2}]		Thickness t [nm]	Roughness Δt [nm]	Nuclear SLD Nb [10^{-4}nm^{-2}]
SiO_2	1.8	0.9	3.97	SiO_2	1.8	0.9	3.97
# 1	3.6	0.6	1.19	# 1	3.5	0.5	1.12
# 2	26.4	1.1	2.39	# 2	26.5	0.9	2.38
# 3	4.3	1.5	2.75	# 3	4.0	1.4	2.90
# 4	47.8	2.1	2.46	# 4(a)	24.5	2.3	2.55
				# 4(b)	29.9	3.9	3.24
# 5	34.3	7.0	5.08	# 5	25.0	6.9	5.30
FF	-	18.0	5.27	FF	-	1.9	5.27

Uncertainties of polarized neutron reflectivity fits

Figures S4 and S5 show histogram plots of the probability vs parameter value which are used to determine parameter uncertainties, and the correlation plots generated from the DREAM Bayesian algorithm in Refl1D[1,2] used for fitting the PNR data in Figure 4 of the main text. The histograms of the density of points visited during the fit (left diagrams) provide a picture of the probability density function for each parameter. The histogram range represents the 95 % credible interval, and the shaded region represents the 68 % credible interval. The green line shows the highest probability observed given that the parameter is restricted to that histogram bin. The correlation plots (right diagrams) display the probability density as a function of each pair of parameters, summing over the remaining parameters, and provides a graphical representation of any correlations and the degree to which the parameters are uniquely determined from the data.

Figure S6 shows the statistically-significant difference between the spin asymmetries at 100 mT and 6 mT. The data points are the subtracted data and the lines are the subtracted asymmetries derived from the fits to the data. The agreement between data and fit values is fairly good, particularly in the low q-range, and is indicative of the accuracy of the PNR fits.

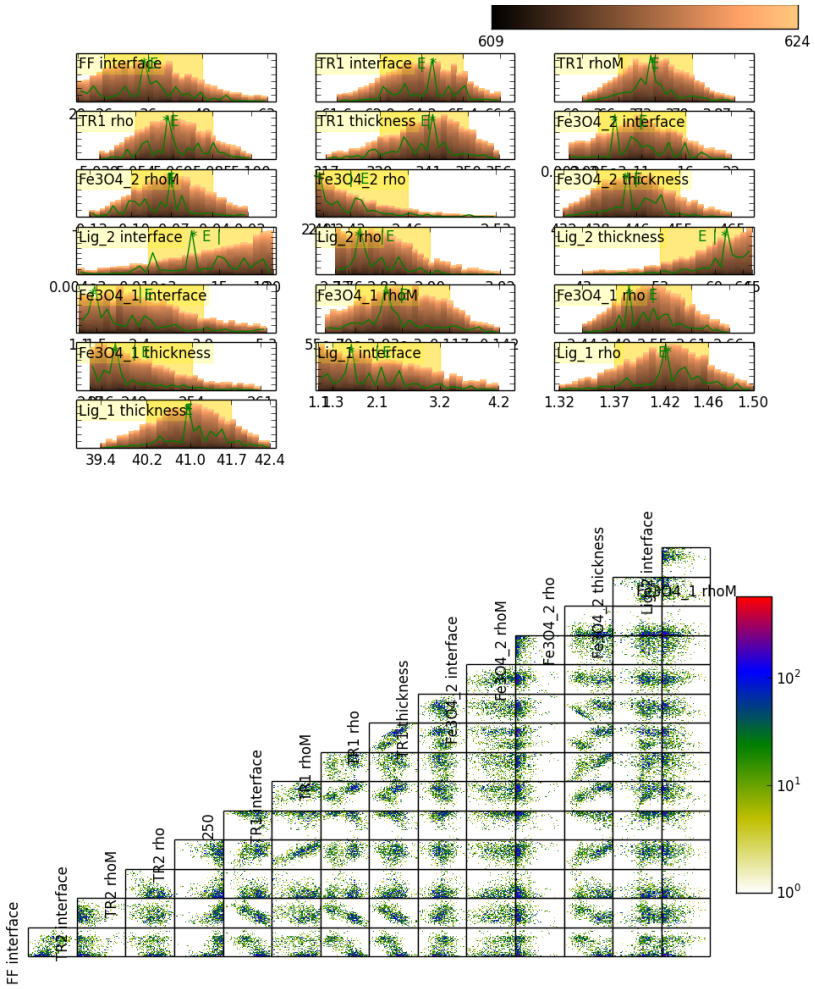

Figure S4: Histogram (top) and correlations (bottom) plots generated by the DREAM Bayesian algorithm in Refl1D used for fitting the polarized reflectivity data taken at 0 mT in Figure 4 of the main text.

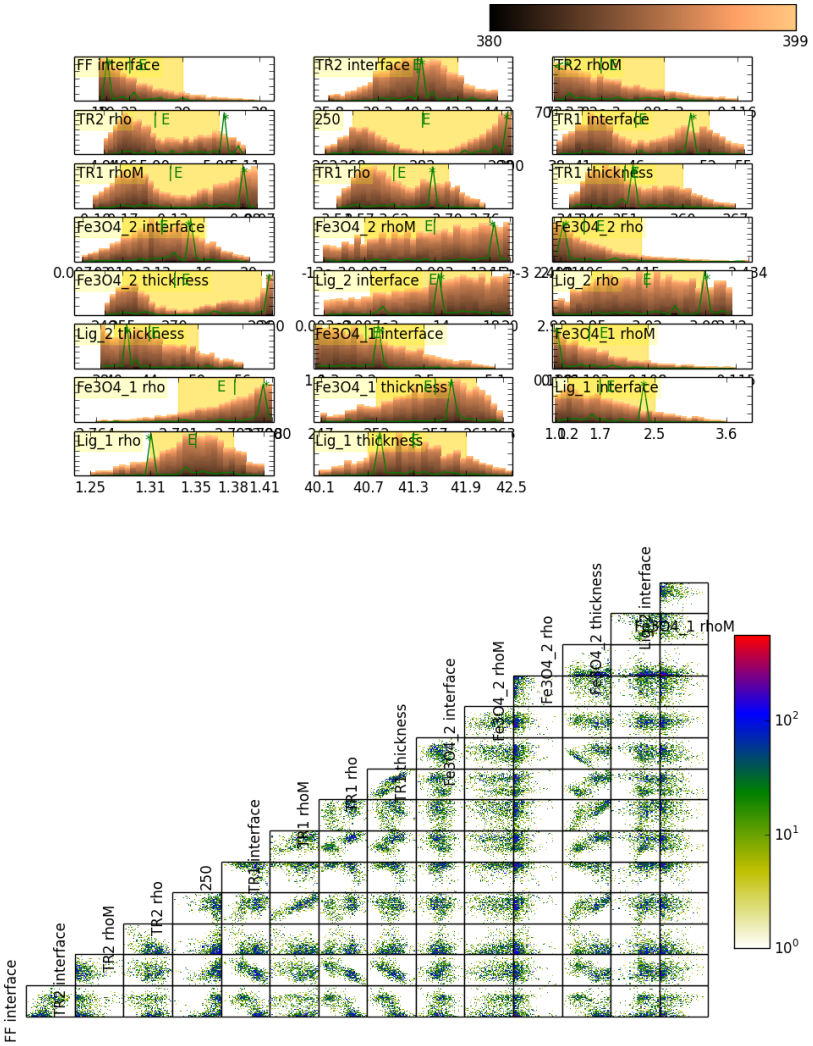

Figure S5: Histogram (top) and correlations (bottom) plots generated by the DREAM Bayesian algorithm in Refl1D used for fitting the polarized reflectivity data taken at 100 mT in Figure 4 of the main text.

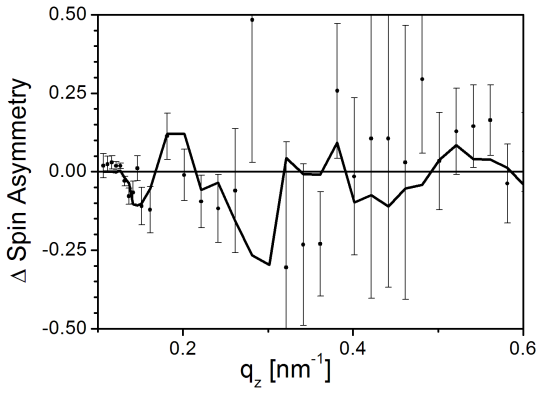

Figure S6: Difference between the spin asymmetry curves taken at 100 mT and 6 mT from Figure 4 (c) and Figure 4 (b) of the main text, respectively. The solid line represents the differences of the calculated spin asymmetry from the fits to the data.

Bulk SLD values

In Table S2 the SLD's of several parameters of the ferrofluid are provided. They can be calculated by using the concentration of magnetite in the solution of 0.15 vol%, the core and core/shell thicknesses of 25 nm and 34 nm, respectively, and the SLD of the ferrofluid (FF) of $\mathrm{Nb_{FF}} = 5.27 \cdot 10^{-4}\mathrm{nm}^{-2}$ (obtained from our fits, see below).

Details of model calculations

To interpret the SLD profile in terms of the arrangement of the particles within the individual layers, we applied a model with hard sphere particle ordering. In this model the core/shell particles are close packed to build a single sheet of truncated particles arranged in a six-fold geometry (see Figure S7). The thickness of the stack corresponds to the core diameter d_c and the core-shell spherical particles within the stack are arranged in a six-fold geometry. The hexagonal unit cell has a lattice parameter equal to the core/shell diameter d_{c+s} and a volume of $V_{uc,tr} = \frac{\sqrt{3}}{2} d_{c+s}^2 d_c$. The volume of the core material corresponds to $V_c = \frac{\pi}{6} d_c^3$ and the shell material contains a volume of $V_s = \frac{\pi}{4} d_c (d_{c+s}^2 - d_c^2)$ which is the result of cutting off from the shell two caps with a volume of $V_{cap} = \frac{\pi}{24}(d_{c+s} - 2d_c)^2(2d_{c+s} + d_c)$ each. This

Table S2: Bulk SLD values of the components of the ferrofluid and other materials as calculated by using Ref. 3.

Material	Structure	Concentration	Nuclear SLD Nb [10^{-4}nm^{-2}]
Components of the ferrofluid:			
Water (84.8% D_2O/15.2% H_2O)	solvent	1.000	5.28
D_2O	solvent 1	0.845	6.33
H_2O	solvent 2	0.151	-0.56
Case 1: core/shell diameter of 34.0 nm			
Ferrofluid particle (41.2% Fe_3O_4/58.8% ligand)	core/shell	0.0036	3.15
Fe_3O_4 core with diameter of 25.3 nm	core	0.0015	6.91
ligand shell with thickness of 4.35 nm	shell	0.0021	0.44
Case 2: core/shell diameter of 38.5 nm			
Ferrofluid particle (28.4% Fe_3O_4/71.6% ligand)	core/shell	0.0053	2.28
Fe_3O_4 core with diameter of 25.3 nm	core	0.0015	6.91
ligand shell with thickness of 6.6 nm	shell	0.0038	0.44
Ferrofluid (composed from above)		1.0000	5.27
Silicon wafer:			
Si	wafer		2.07
SiO_2	native oxide		3.97

results in concentrations of the core material of

$$c_c^{cp,tr} = \frac{\pi\sqrt{3}}{9} \cdot \frac{{d_c}^2}{{d_{c+s}}^2} \tag{1}$$

and the concentration of the shell material of

$$c_s^{cp,tr} = \frac{\pi\sqrt{3}}{6} \cdot \frac{(d_{c+s}^2 - d_c^2)}{d_{c+s}^2} \tag{2}$$

SLD values were calculated for the following cases: (1) core diameter d_c = 25.3 nm and center-to-center dimer distance d_d = 34.0 nm as determined from the SANS fits shown in Table 1 in the main text of the paper, and (2) core diameter d_c = 25.3 nm and center-to-center distance d_{c+s} = 38.5 nm as determined from the SANS data for a single nanoparticle.

By using these volume fractions and the material SLD values, we derived the model SLD values for the close packed layers with the different dimensions, given in Figure S7.

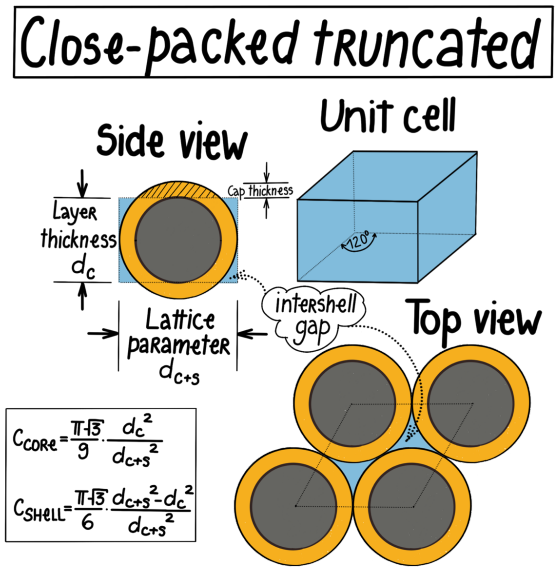

Figure S7: Model for ordering of truncated hard-sphere core/shell particles in a close-packed sixfold arrangement.

References

(1) Kienzle, P.; Maranville, B.; O'Donovan, K.; Ankner, J.; Berk, N.; Majkrzak, C. Retrieved December 12, 2017 from the World Wide Web. `https://www.nist.gov/ncnr/reflectometry-software`.

(2) Dura, J. A.; Rus, E. D.; Kienzle, P. A.; Maranville, B. B. In *Nanolayer Research: Methodology and Technology for Green Chemistry*; Imae, T., Ed.; Elsevier, 2017; Vol. 12; Chapter 5: Nanolayer Analysis by Neutron Reflectometry, pp 155– 202.

Table S3: Model SLD values calculated for a layer of hexagonal close-packed particles. In the model calculation the included volume is limited by the tangent planes touching the monolayer of particle cores above and below, i.e. with a thickness of $d_c = 25$ nm. It was assumed that either water or shell material fills the interstitial gaps between the spherical shells within these limiting planes. The calculation was performed for two different shell thicknesses.

Model	thickness [nm]	d_{c+s} [nm]	c_{core}	c_{shell}	c_{water}	SLD
			Volume fractions			Nb [10^{-4}nm^{-2}]
Water in intershell gaps						
	25.3	34.0	0.33	0.40	0.27	3.87
	25.3	38.5	0.26	0.52	0.22	3.21
Shell material in intershell gaps						
	25.3	34.0	0.33	0.67	0	2.56
	25.3	38.5	0.26	0.74	0	2.13